

ARTICLE

Open Access

Triplet-radical spin entanglement: potential of molecular materials for high-temperature quantum information processing

Lin Ma^{1,2,3}, Jiawei Chang^{1,2,3}, Qiuyuan Chen^{1,2,3}, Taoyu Zou⁴, Wei Wu⁵ and Hai Wang^{1,2}

Abstract

Recently, spin-bearing molecules have been experimentally demonstrated to have great potential as building blocks for quantum information processing due to their substantial advantages including tunability, portability, and scalability. Here, we propose a theoretical model based on the theory of open quantum systems for spin dynamics in a molecule containing one radical, which can interact with the triplet state arising from another part of the molecule owing to optical excitation and intersystem crossing. With the initial state being a classical mixture of a radical $\frac{1}{2}$ -spin, the exchange interaction between the radical and the triplet produces a spin coherent state, which could potentially be used for a qubit-qutrit quantum entangling gate. Our calculations for the time-resolved electron paramagnetic resonance spectra showed good qualitative agreement with the related experimental results for radical-bearing molecules at high temperature (~ 77 K, the boiling point of liquid nitrogen). This work therefore lays a solid theoretical cornerstone for optically driven quantum gate operations in radical-bearing molecular materials, aiming toward high-temperature quantum information processing.

Introduction

Great progress has been achieved in building quantum information processing (QIP) devices, such as by using superconducting circuits^{1–3}. Although superconducting circuits have many advantages such as simple configurability, and up to 53 superconducting qubits have been fabricated and connected¹, they have a short decoherence time and need to be kept at a very low temperature. Currently, most QIP devices indispensably rely on the control of ultralow temperatures down to millikelvin². Hence, quantum gate operations at higher temperatures are still an inevitable obstacle to overcome for a practical

QIP device⁴. Optical excitations, especially in organic materials, could be one of the solutions, offering larger energy scales for coherent interactions against incoherent thermal noise due to the high temperature (~ 77 K, the boiling point of liquid nitrogen)^{5–7}. By using optical excitations, we can also avoid the decoherence induced by the external electrodes conventionally used for the control of electrons⁸. Moreover, the spins in organic molecules can have a long spin-lattice relaxation time (T_1) due to the weak hyperfine interaction and spin-orbit coupling⁹ and a long spin-spin relaxation time (T_2 , characterizing the transverse relaxation process owing to spin-spin interactions) because of the controllably weak coupling between spins. For example, the T_1 time for diluted copper-phthalocyanine (CuPc) can reach microseconds at 200 K¹⁰. In the meantime, the T_2 time for diluted CuPc, which is very important for fault-tolerant quantum computing, is on the order of microseconds at 100 K, comparable to the nitrogen-vacancy center in diamond¹⁰. For some systems, T_2 is much shorter than T_1 , but if there

Correspondence: Taoyu Zou (taoyuzou@sina.com) or Wei Wu (wei.wu@ucl.ac.uk)
Hai Wang (wanghai_lab@sina.com)

¹Yunnan Key Laboratory of Metal-Organic Molecular Materials and Devices, Kunming University, Kunming, Yunnan Province, P. R. China

²Key Laboratory of Yunnan Provincial Higher Education Institutions for Organic Optoelectronic Materials and Devices, Kunming University, Kunming, Yunnan Province, P. R. China

Full list of author information is available at the end of the article
These authors contributed equally: Lin Ma, Jiawei Chang

© The Author(s) 2022



Open Access This article is licensed under a Creative Commons Attribution 4.0 International License, which permits use, sharing, adaptation, distribution and reproduction in any medium or format, as long as you give appropriate credit to the original author(s) and the source, provide a link to the Creative Commons license, and indicate if changes were made. The images or other third party material in this article are included in the article's Creative Commons license, unless indicated otherwise in a credit line to the material. If material is not included in the article's Creative Commons license and your intended use is not permitted by statutory regulation or exceeds the permitted use, you will need to obtain permission directly from the copyright holder. To view a copy of this license, visit <http://creativecommons.org/licenses/by/4.0/>.

is only an amplitude damping channel, then T_2 is equal to $2T_1$. A long spin coherence time in vanadyl-Pc (1.04 microseconds) has also been observed even at room temperature, suggesting the potential of radical-bearing molecules for quantum gate operations¹¹. In addition, organic molecules have major potential for QIP due to their scalability, portability, and tunability^{6,9}. Recently, Bayliss et al. addressed the molecular spins for QIP in organic materials, using a small complex consisting of a chromium ion coordinated by aryl ligands⁶. The authors demonstrated the initialization, coherent control, and read-out of spin qubits by using optical excitations. In addition, the quantum teleportation of spin states at 85 K was demonstrated experimentally in a covalent donor-acceptor radical pair system¹². More importantly, the incorporation of organic radicals (spin- $\frac{1}{2}$, a natural candidate for qubits) into the QIP molecular architecture and further scalability improvements, facilitated by chemical synthesis and molecular engineering, are easier than their traditional inorganic counterparts¹³.

For radical-bearing molecules, the long-lived triplet (spin-1) can be formed by optical excitations and inter-system crossing (ISC, from the singlet excited state to the triplet ground state)¹⁴, which can interact via exchange interactions coherently with the radical spin. The triplet plays a role not only as a qutrit (a 3-level quantum system), which can lead to increased security, greater channel capacities, and more efficient gate operations⁷, but also a coupler for controlling the interaction between radicals¹⁵. Spin states such as a quartet (one radical coupled with a triplet), as shown in Fig. 1, or even higher spin states¹⁶ with multiple radicals can be produced, which have been observed by time-resolved electron paramagnetic resonance (TR-EPR) spectroscopy^{15,17–22}. The electron spin coherence therein due to the exchange interaction at high temperature can be used for quantum gate operations. This exchange interaction, the strongest short-range interaction between electron spins, plays an essential role in spin-based QIP for producing coherence^{23–25}. Teki et al. performed experimental and theoretical works on the exchange-coupled doublet-triplet molecular system^{26–28}. The authors' research focused on spin dynamics, spin polarization, and population transfers. The theoretical methods used therein for dealing with decoherence due to the environment are essentially semiclassical, whereas the system Hamiltonian is quantum²⁶. Previously, the interaction between the doublet and triplet was studied theoretically based on perturbation theory up to the second order. These studies indicated the dependence of spin polarizations on the exchange interaction, magnetic field, and zero-field splitting. An interesting conclusion therein is that the net spin polarization for the doublet can still survive even after triplet relaxation^{29,30}. In addition, CuPc molecules

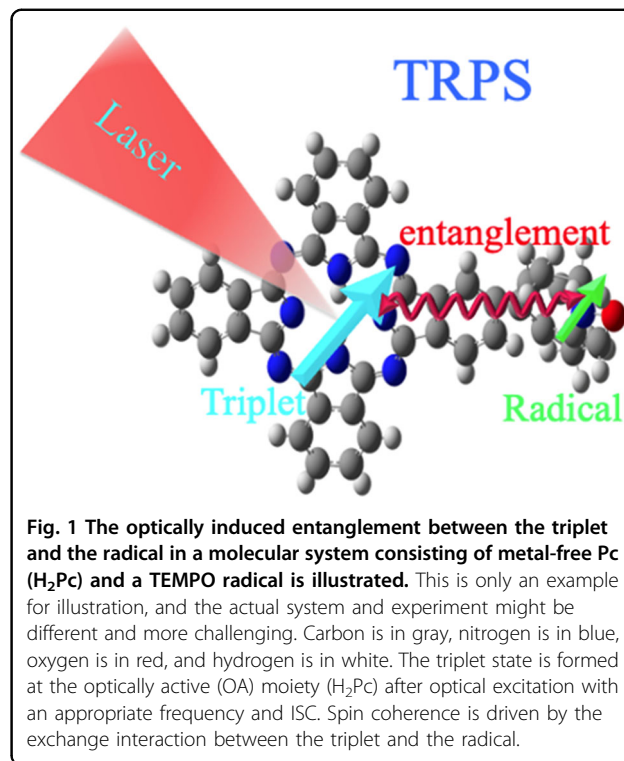


Fig. 1 The optically induced entanglement between the triplet and the radical in a molecular system consisting of metal-free Pc (H₂Pc) and a TEMPO radical is illustrated. This is only an example for illustration, and the actual system and experiment might be different and more challenging. Carbon is in gray, nitrogen is in blue, oxygen is in red, and hydrogen is in white. The triplet state is formed at the optically active (OA) moiety (H₂Pc) after optical excitation with an appropriate frequency and ISC. Spin coherence is driven by the exchange interaction between the triplet and the radical.

could serve as a good platform for optically controlled spin coherence at high temperature, as suggested by density functional theory calculations for the exchange interaction between the localized spin on the Cu ion and the triplet³¹. Theoretical validation of the optically controlled spin coherence in radical-bearing molecules can open a new avenue to achieve high-temperature QIP; thus, a general open quantum system model is mandatory for the realization of QIP at temperatures far above millikelvin.

In this work, we proposed a general open quantum system model for triplet-radical pair systems (TRPSs), such as organic molecules containing one radical, as illustrated in Fig. 1. Here, we assumed that the molecules were sufficiently far apart such that we were equivalently dealing with an isolated single molecule consisting of a radical and a triplet, provided the molecular densities could still ensure a good signal in the TR-EPR experiment. We therefore neglected the explicit T_2 effect in this work. Our numerical results based on the Markovian approximation within the weak coupling limit were qualitatively in good agreement with recent TR-EPR experiments on TRPSs³². Most importantly, our work suggested the feasibility of high-temperature quantum gate operations based on radical-bearing molecules.

System description and theoretical method

In TR-EPR experiments, the environment in which spin-bearing molecules are usually exposed is important

for the description of spin dynamics, such as lattice vibrations (crucial for determining spin-lattice relaxation times). At temperatures even above the boiling point of liquid nitrogen, the spin-lattice relaxation time of a radical spin is typically \sim microsecond, as in CuPc and N@C₆₀¹⁰. ISC normally happens faster (transition time \sim nanosecond or transition rate \sim 10 mT) than spin-lattice relaxation owing to the spin-orbit interaction. ISC results in a very slow relaxation from the triplet state back to the singlet ground state, and the phosphorescence lifetime is \sim millisecond. The static magnetic field is on the order of 100 mT, as found, for example, in typical X-band EPR spectroscopy (\sim 9.5 GHz). Therefore, the Markovian description in the theory of open quantum systems (the weak coupling limit) could be a good approximation to describe the spin dynamics in TRPSs exposed to the environment³³. Here, we established an effective spin Hamiltonian and a set of quantum jump operators, set up Liouville equations (and the corresponding superoperators—Liouvillians), and calculated the time evolution of the density matrices and the TR-EPR spectra.

Effective Hamiltonian

The effective spin Hamiltonian of a TRPS reads

$$\hat{H}_{\text{TRPS}} = g_t \mu_B \mathbf{B} \cdot \hat{\mathbf{T}} + g_r \mu_B \mathbf{B} \cdot \hat{\mathbf{s}} + J \hat{\mathbf{s}} \cdot \hat{\mathbf{T}} + D \hat{T}_z^2 + E (\hat{T}_x^2 - \hat{T}_y^2) \quad (1)$$

$\hat{\mathbf{T}}$ is the triplet spin-1 of the optically active (OA) moiety and $\hat{\mathbf{s}}$ the radical $\frac{1}{2}$ -spin. The addition of the two spins leads to a total spin of $\frac{1}{2}$ (a doublet, with a multiplicity of 2) and $\frac{3}{2}$ (a quartet, with a multiplicity of 4). The first two terms are the Zeeman energies for the triplet and the radical with a static magnetic field of \mathbf{B} , respectively. g_t is the g-factor of the triplet spin, while g_r is the radical spin. The third term is the exchange interaction (J) between the radical and the triplet. D and E are the zero-field splitting (ZFS) for the triplet, as shown in the last two terms. The triplet and radical spins are entangled when J is comparable with or larger than D and E .

If we combine the optical field with the effective Hamiltonian above (Eq. 1) and use the rotating wave approximation (RWA)³⁴, we have

$$\hat{H}_{\text{TRPS}}^{\text{OPT}} = |T\rangle \langle T| \hat{H}_{\text{TRPS}} + |S_1\rangle \langle S_1| [g_r \mu_B \mathbf{B} \cdot \hat{\mathbf{s}}] + |S_0\rangle \langle S_0| [g_r \mu_B \mathbf{B} \cdot \hat{\mathbf{s}}] + V(|S_1\rangle \langle S_0| + |S_0\rangle \langle S_1|) \quad (2)$$

for a TRPS interacting with the optical field V . Here, S_0 represents the singlet ground-state manifold, S_1 is the excited singlet, and T is the triplet. The first term represents the interaction in a triplet manifold. The second and third terms are for the Zeeman energies of the

radical when the OA moiety is in the singlet ground and excited states, respectively. The last term describes the optical excitation; here, V is the optical transition matrix element between the ground and excited singlet states (S_0 and S_1 , respectively). Note that we used the bases $|\frac{1}{2}, \frac{1}{2}\rangle$ and $|\frac{1}{2}, -\frac{1}{2}\rangle$ for the radical spin and $|1, 1\rangle$, $|1, 0\rangle$, and $|1, -1\rangle$ for the triplet spin (the spin states are written in the form of $|s, m_s\rangle$). Compared with the traditional convention for the triplet ($|+\rangle$, $|0\rangle$, and $|-\rangle$), this choice of bases was beneficial for the QIP representation of the quantum states³⁵. In addition, the molecular orientation has a crucial effect on the quantum state populations and EPR spectra^{36,37}. In practice, the EPR spectra need to be simulated as the averaging effect due to the randomly distributed molecular orientations relative to the static magnetic field direction. However, in this work, we assumed that the molecular principal axis was along the z-direction of the static magnetic field; i.e., we neglected the orientation effect at the moment. In the future, we would like to perform theoretical work on the molecular orientation effect. Therein, we will compute and evaluate the molecular orientation effect on the quantum state populations and EPR spectra and the powder averaging for the random distribution of molecular orientations. We will also take into account the molecular aggregation effect determined by the molecular density and distributions (closely related to the spin-spin interactions between molecules), which is also important for the EPR spectra of spin-bearing molecules³⁷.

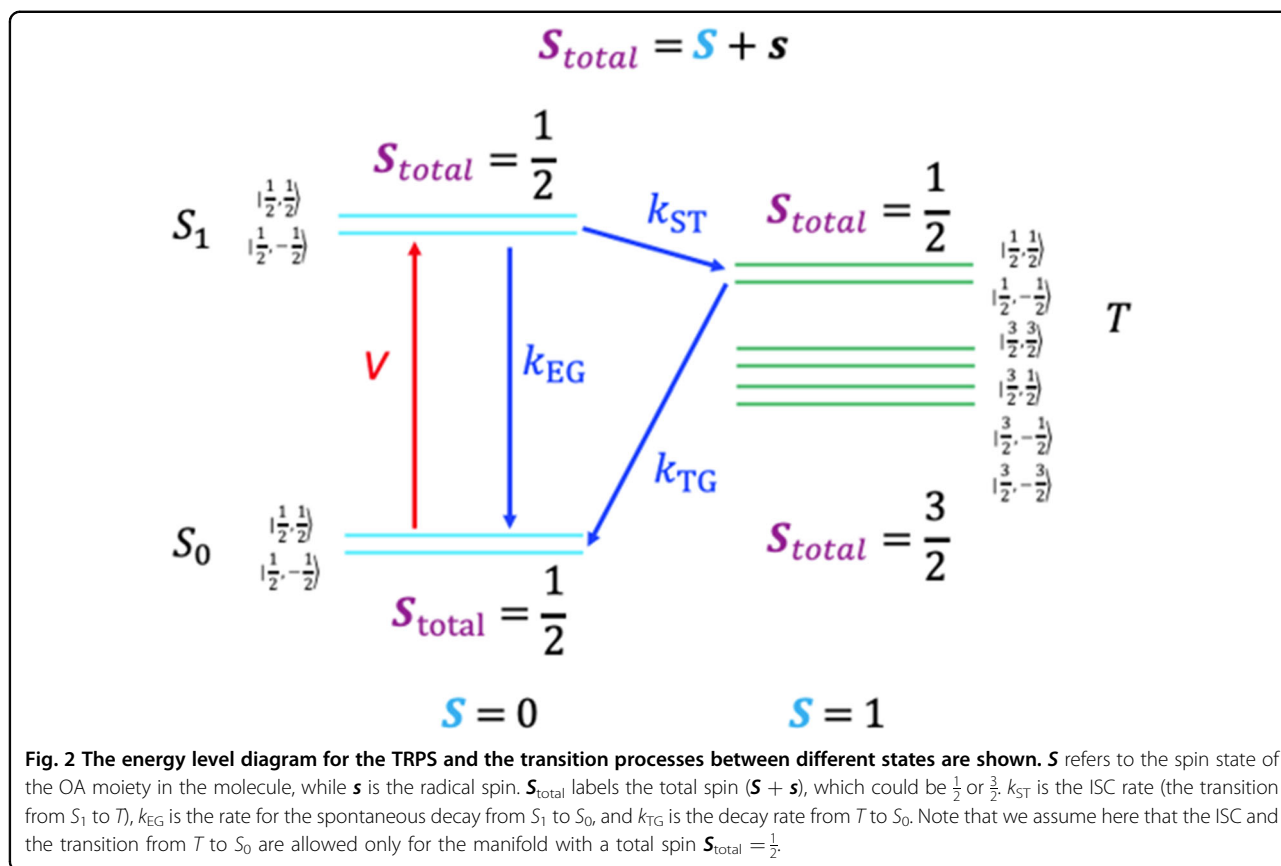
Quantum jump operators

For the incoherent processes, we took into account the spin relaxations, the spontaneous decay of the singlet excited state, and the crossovers between the singlet excited and triplet states (ISC and the slow decay from the triplet state to singlet ground state). Figure 2 shows the transition processes in TR-EPR experiments for the TRPS. Therein, k_{ST} is the transition rate for ISC (from the singlet excited state to the triplet state), k_{EG} is the rate for the spontaneous decay from the singlet excited to ground state and k_{TG} is the rate for the decay from the triplet to singlet ground state.

As shown in Fig. 2, the energy level diagram of different spin configurations, optical excitations and different relaxation and decay processes were included. We listed the Liouvillian operators that describe quantum jumps (incoherent processes) below. The superoperators constructed by the Lindblad operators were as follows:

$$\hat{L}_i \hat{\rho} = \sum_{\mu=1}^{n_i} \gamma_{\mu}^i \left[\hat{l}_{\mu}^i \hat{\rho} \hat{l}_{\mu}^{i\dagger} - \frac{1}{2} \left\{ \hat{\rho}, \hat{l}_{\mu}^{i\dagger} \hat{l}_{\mu}^i \right\} \right] \quad (3)$$

Here, $\hat{\rho}$ is the density matrix. The square bracket is the commutator, and the curly bracket is the anticommutator.



For a TRPS, $i = 1$ to 5 (labeling different incoherent processes), the rate of the incoherent processes is described as γ_{μ}^i , where μ labels different operators. \hat{L}_1 with $n_1 = 3$ is used to describe the radical spin- $\frac{1}{2}$ relaxation as follows: $\hat{l}_1^+ = \hat{s}^+$ (spin- $\frac{1}{2}$ raising operator), $\hat{l}_2^- = \hat{s}^-$ (spin- $\frac{1}{2}$ lowering operator), and $\hat{l}_3^z = \hat{s}_z$ (the z -component of spin- $\frac{1}{2}$). The \hat{s}_z operator is responsible for the pure dephasing of quantum states, whereas \hat{s}^+ and \hat{s}^- are responsible for random jumps. \hat{L}_2 with $n_2 = 8$ is used as a superoperator to describe the relaxation of the triplet state. We used the eight Gell-Mann matrices for these operators. Note that we implicitly included the transverse relaxation process corresponding to the T_2 time in our Lindblad formalism through the pure dephasing Lindblad operators for both the radical and the triplet. Here, we accounted for the ISC; however, we assumed here that the total spin angular momentum was conserved, i.e., $S_{total} = \frac{1}{2}$, thus obtaining the following operators. \hat{L}_3 with $n_3 = 2$ is the superoperator describing the transition from the single excited state to the triplet state; $\hat{l}_1^3 = |\frac{1}{2}, \frac{1}{2}\rangle_T \langle \frac{1}{2}, \frac{1}{2}|_{S_1}$ and $\hat{l}_2^3 = |\frac{1}{2}, -\frac{1}{2}\rangle_T \langle \frac{1}{2}, -\frac{1}{2}|_{S_1}$. Similarly, we have \hat{L}_4 with $n_4 = 2$, which is the superoperator for the transition from the singlet excited to singlet

ground state; $\hat{l}_1^4 = |\frac{1}{2}, \frac{1}{2}\rangle_{S_0} \langle \frac{1}{2}, \frac{1}{2}|_{S_1}$ and $\hat{l}_2^4 = |\frac{1}{2}, -\frac{1}{2}\rangle_{S_0} \langle \frac{1}{2}, -\frac{1}{2}|_{S_1}$, corresponding to spontaneous decay. \hat{L}_5 where $n_5 = 2$ is the superoperator that describes the transition from the triplet state to the singlet ground state; $\hat{l}_1^5 = |\frac{1}{2}, \frac{1}{2}\rangle_{S_0} \langle \frac{1}{2}, \frac{1}{2}|_T$ and $\hat{l}_2^5 = |\frac{1}{2}, -\frac{1}{2}\rangle_{S_0} \langle \frac{1}{2}, -\frac{1}{2}|_T$. γ_{μ}^i will be parametrized later.

The spin Hamiltonian operator and quantum jump operator (implemented through the Lindblad equation) can then be combined into the Liouville equation, or equivalently the Liouvillian formalism³³. Therefore, the total Liouvillian superoperator is written as

$$\hat{Q}\hat{\rho} = -i[\hat{H}_{TRPS}^{OPT}, \hat{\rho}] + \left[\sum_i \hat{L}_i \right] \hat{\rho} \quad (4)$$

Here, the first part is the coherent interaction from the effective spin Hamiltonian and optical field (see Eq. 2). The second part includes the incoherent processes associated with the relaxations and crossovers between states (see Eq. 3). Therefore, we obtained a 10 by 10 Hamiltonian matrix (2 for the singlet ground state with the spin- $\frac{1}{2}$ radical, 2 for the singlet excited states with the spin- $\frac{1}{2}$

radical, 6 for the triplet state with radical), leading to a 100 by 100 Liouvillian matrix.

Linear response theory for TR-EPR spectra

For TR-EPR spectra, we adopted and generalized phenomenally the formalisms presented in refs. 38,39. Based on linear response theory, the intensities of the TR-EPR spectra were calculated as follows:

$$I(t, \omega) = \left| \text{Tr} \left\{ \hat{\rho}(t) [\hat{T}_x + \hat{s}_x] \left[i\hat{\Omega} - \omega I \right]^{-1} [\hat{T}_x + \hat{s}_x] \right\} \right| \quad (5)$$

Here, $\hat{\rho}(t)$ is the time-dependent density matrix. $\hat{T}_x + \hat{s}_x$ is the x -component of the total spin. ω is the frequency of the microwave field. I is the identity matrix. $\hat{\Omega}$ is the superoperator (see Eq. 4).

Results and discussion

Here, we assumed that the radical and triplet had comparable spin-lattice relaxation rates, which were at ~MHz levels at the boiling point of liquid nitrogen¹⁰. ISC was fast (at a rate ~0.1 GHz). The system decayed very slowly from the triplet to the singlet ground state (at a rate ~kHz). We varied these parameters to carefully observe the effects of the spin relaxation rates on the TR-EPR spectra. Another important parameter was the exchange interaction between the radical and the triplet, which could not only be calculated by density functional theory but also estimated by fitting the experimental EPR spectra. We used millitesla (mT) as the unit of energy and relaxation rates throughout the paper. Here, we explored a set of values for the exchange interaction (either

ferromagnetic or antiferromagnetic), including -10, -20, 20, and 50 mT. Our model could be used to predict the time evolution of density matrices and, more importantly, the two-dimensional TR-EPR spectra in the time and magnetic field domains.

The parameters used for calculations

Here, for ZFS, we assumed that D was 10 mT and E was 1 mT, which are the typical values for molecules¹⁶. To simplify our parameters, we assumed that $g_r = g_t = 2.0$. We also assumed that $\gamma_i^1 (i = 1 - 3) = k_R$, $\gamma_i^2 (i = 1 - 8) = k_T$, $\gamma_1^3 = \gamma_2^3 = k_{ST}$, $\gamma_1^4 = \gamma_2^4 = k_{EG}$, and $\gamma_1^5 = \gamma_2^5 = k_{TG}$. Here, k_R and k_T are the relaxation rates for the radical and the triplet, respectively. The initial density matrix was chosen to be the thermalized classical mixture for the radical, i.e., $\hat{\rho}_0 = \frac{1}{2} \left(\left| \frac{1}{2}, \frac{1}{2} \right\rangle_{S_0} \left\langle \frac{1}{2}, \frac{1}{2} \right|_{S_0} + \left| \frac{1}{2}, -\frac{1}{2} \right\rangle_{S_0} \left\langle \frac{1}{2}, -\frac{1}{2} \right|_{S_0} \right)$.

The spin entanglement generation process can be elucidated by comparing our calculations with experiments. In the coherent part, we had $D = 10$ mT, $E = 1$ mT, $J = -10$ mT, and $V = 10$ mT. We also estimated the incoherent parameters for the high temperature as follows: $k_R = 0.1$ mT, $k_T = 0.1$ mT, $k_{ST} = 10$ mT, $k_{TG} = 0.0001$ mT, and $k_{EG} = 0.01$ mT. The magnetic field ranged between 280 mT and 420 mT.

Time evolution of the density matrix

First, we simulated the time evolution of the density matrix up to ~200 ps from time 0, when an optical excitation was applied. As shown in Fig. 3, we computed the time evolution of the populations (the diagonal terms of the density matrix, for the excited states $|0, 0\rangle_e \left| \frac{1}{2}, \frac{1}{2} \right\rangle$, $|1, 0\rangle \left| \frac{1}{2}, \frac{1}{2} \right\rangle$, and $|1, -1\rangle \left| \frac{1}{2}, \frac{1}{2} \right\rangle$, and the ground state

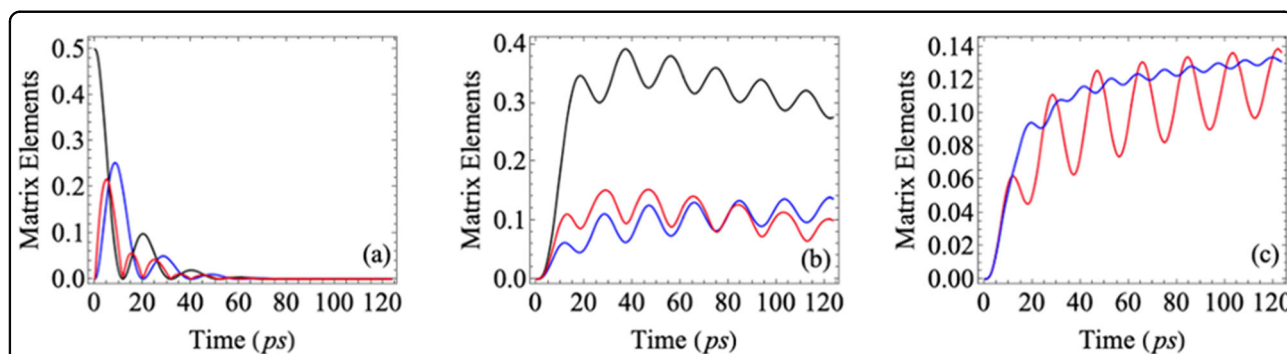


Fig. 3 The time evolutions of the matrix elements are shown. **a** The populations of spin state $|0, 0\rangle_g \left| \frac{1}{2}, \frac{1}{2} \right\rangle$ are shown in blue, while spin state $|0, 0\rangle_e \left| \frac{1}{2}, \frac{1}{2} \right\rangle$ is shown in black. The off-diagonal term between the above two states is shown in red. **b** The populations of the spin states $|1, 0\rangle \left| \frac{1}{2}, \frac{1}{2} \right\rangle$ and $|1, 1\rangle \left| \frac{1}{2}, -\frac{1}{2} \right\rangle$ are shown in blue and black, respectively, and the off-diagonal term between the two states is shown in red. All the matrix elements of these states shown here exhibit Rabi oscillation, implying coherence induced by the optical excitations. All the parameters used are listed in the main text. **(c)** The time evolutions of the populations of the spin state $|1, 0\rangle \left| \frac{1}{2}, \frac{1}{2} \right\rangle$ are shown. The red curve is for the exchange interaction $J = -10$ mT and the blue curve for $J = -20$ mT. We can see that within this energy range, the oscillation frequency for the population increases with the exchange interaction. This behavior suggests a correlation between coherent oscillations and the exchange interaction.

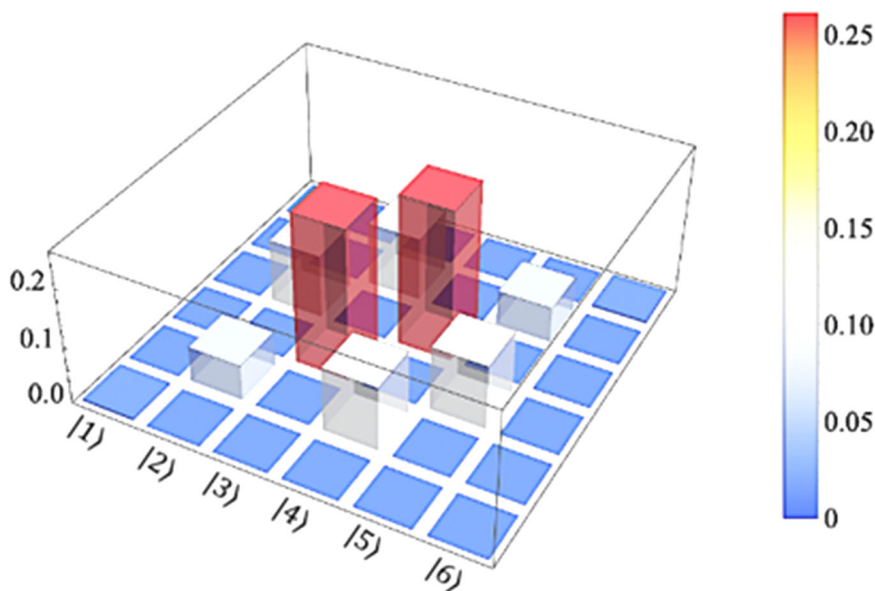


Fig. 4 The tomography of the density matrix for the sextet at the early stage ($T = 6.2$ ps) is shown. Nonzero off-diagonal terms (coherence) are clearly shown in gray.

$|0, 0\rangle_g|\frac{1}{2}, \frac{1}{2}\rangle$, which corresponded to $\rho_{11}, \rho_{44}, \rho_{66}$, and ρ_{99} , respectively). Here, the first bracket was for the singlet/triplet manifold (the singlet excited state labeled by e , the ground state by g) of the OA moiety of the molecule, and the second bracket was for the radical spin. The absolute values of the corresponding off-diagonal terms ($|\rho_{19}|$ and $|\rho_{46}|$), which characterized the coherence, were calculated.

We can see the Rabi oscillations of the populations and the off-diagonal terms for the states in Fig. 3, which suggested that spin coherence could be produced by using this optically driven process, starting from a classical mixture state of the radical spin. The resulting entanglement between the radical and the triplet provides the foundation for the QIP application of the proposed molecular architecture. The populations of $|0, 0\rangle_e|\frac{1}{2}, \frac{1}{2}\rangle$ and $|0, 0\rangle_g|\frac{1}{2}, \frac{1}{2}\rangle$ (the blue and black curves in Fig. 3a, respectively) oscillated in the beginning but decayed very fast. These oscillatory processes for the states $|0, 0\rangle_e|\frac{1}{2}, \frac{1}{2}\rangle$ and $|0, 0\rangle_g|\frac{1}{2}, \frac{1}{2}\rangle$ were mainly driven by the external optical excitations. The oscillating populations for the states $|1, 0\rangle|\frac{1}{2}, \frac{1}{2}\rangle$ and $|1, 1\rangle|\frac{1}{2}, -\frac{1}{2}\rangle$ and the off-diagonal term (the blue, black, and red curves in Fig. 3b, respectively) suggested that spin coherence was driven by the exchange interaction and the external optical excitations, leading to the entangled state between spin- $\frac{1}{2}$ and the triplet. From these analyses, with the chosen parameters, we also observed that the populations were cumulated to the sextet states (the right-hand-side part in Fig. 2) formed by the radical and the triplet because of a fast ISC rate and a strong optical driving field but a slow decay back down to the singlet ground state. However, the coherence

eventually vanishes after removing the optical driving, owing to the decay of the triplet to the singlet ground state.

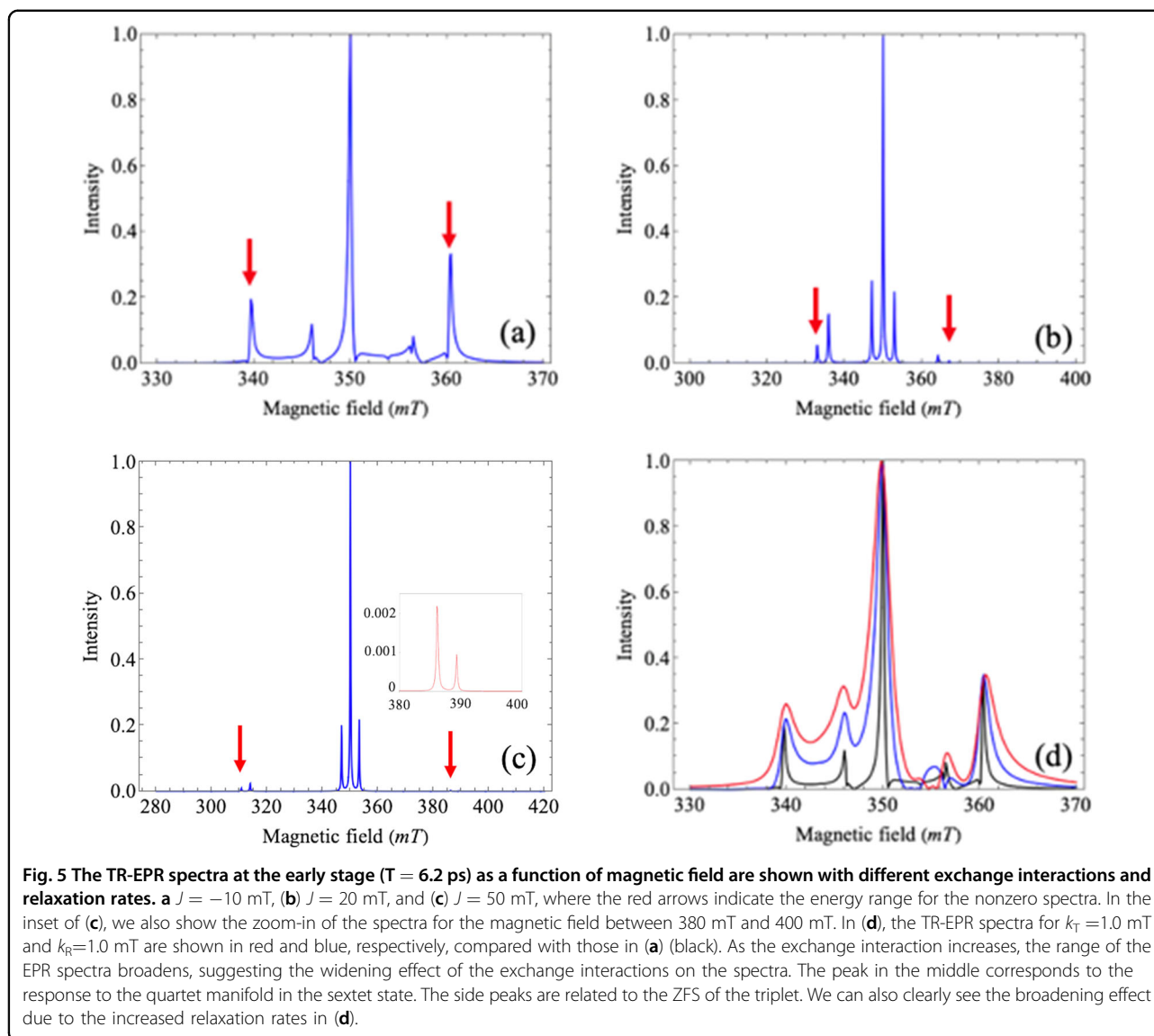
As shown in Fig. 3c, we compared the time evolutions of the population of the spin state $|1, 0\rangle|\frac{1}{2}, \frac{1}{2}\rangle$ for the exchange interaction equal to -10 mT (the red curve) and -20 mT (the blue curve). The oscillation frequency increased with increasing magnitude of the exchange interaction. This comparison suggested that the oscillatory behavior of the populations (and coherence) for the states $|1, 0\rangle|\frac{1}{2}, \frac{1}{2}\rangle$ and $|1, 1\rangle|\frac{1}{2}, -\frac{1}{2}\rangle$ was driven mainly by the exchange interaction, assisted by the optical driving field.

Figure 4 presents the tomography of the sextet density matrix at the early stage ($T = 6.2$ ps), which clearly shows the nonzero off-diagonal terms (coherence) after optical excitation. Here, $|1\rangle = |1, 1\rangle|\frac{1}{2}, \frac{1}{2}\rangle$, $|2\rangle = |1, 0\rangle|\frac{1}{2}, \frac{1}{2}\rangle$, $|3\rangle = |1, -1\rangle|\frac{1}{2}, \frac{1}{2}\rangle$, $|4\rangle = |1, 1\rangle|\frac{1}{2}, -\frac{1}{2}\rangle$, $|5\rangle = |1, 0\rangle|\frac{1}{2}, -\frac{1}{2}\rangle$, and $|6\rangle = |1, -1\rangle|\frac{1}{2}, -\frac{1}{2}\rangle$.

TR-EPR spectra

The response function of the open quantum system was the essential part of our TR-EPR simulations, as shown in Eq. 5.

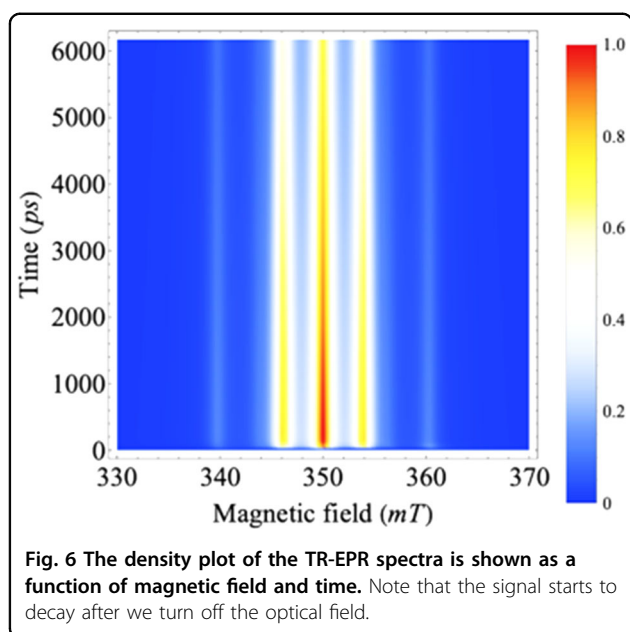
As shown in Fig. 5, we computed the TR-EPR spectra at the early stage of the evolution ($T = 6.2$ ps). As the exchange interaction increased, i.e., $J = -10$ mT, 20 mT, and 50 mT for Fig. 5 (a-c), respectively, we observed a widening range of the EPR spectra. Some of the side peaks stemmed from the triplet spin anisotropy characterized by D and E . On the other hand, the outer peaks far from the



middle were attributed to the exchange interaction. The central peaks were from the quartet components (the total spin = $\frac{3}{2}$) when the spin- $\frac{1}{2}$ and triplet were coupled. Previous studies assigned the lower-energy peaks to the ground state and the middle- and higher-energy peaks to the excited states¹⁶, which implies that the gaps between these peaks will become larger as we increase the exchange interaction. Hence, the widening of the spectral range with the exchange interaction as determined by our calculations was consistent with this picture¹⁶. In Fig. 5 (d), we used the same parameters as in Fig. 3 but increased the magnitudes for k_R and k_T to 1 mT. We can see that the line widths of the EPR spectra were broadened as these processes were incoherent. In addition, compared with the previous work for the experiments on ZnTPP-3-Nopy and MgTPP-Nitpy by Ishii et al.⁴⁰ and

porphyrin-trityl systems evaluated by Nolden et al.³³, we had very good qualitative agreement with the experimental TR-EPR spectra therein.

Figure 6 shows a two-dimensional density plot of the calculated TR-EPR spectra (by using the parameters in Fig. 3) as a function of the magnetic field and time. Here, we turned on the optical field from time = 0 to 6.2 ps and then switched it off to observe the time evolution. As shown in Fig. 6, the TR-EPR spectra signals became stronger as the time evolved within this time range (from 0 to 6.2 ps) but decayed without optical driving. The T_2 process has been implicitly included in our Lindblad formalism, such as the pure dephasing Lindblad operators. However, based on the work here, it is also worth accounting explicitly for the T_2 process in our model and combining the modeling methodology in EasySpin with



the theory of open quantum systems used here³⁶. This work will be carried out in the future and presented in a separate publication. In this forthcoming work, we will also extend the simulation time scale to at least nanoseconds to observe the evolution of entanglement, which is very sensitive to the T_2 time.

Conclusions

In summary, we proposed a general model for the spin dynamics and entanglement of a triplet-radical-pair molecular system based on the Markovian approximation in the theory of open quantum systems. The spin entanglement, implied by the Rabi oscillation characteristics of the density matrix elements owing to the exchange interaction between the triplet and the radical, could be manipulated and controlled by using optical excitations. The computed TR-EPR spectra based on the realistic experimental parameters for organic molecules were qualitatively in good agreement with those from previous experiments on radical-bearing molecules, which theoretically demonstrated a potential route to realize quantum gate operation between qubits and optically accessible qutrits by using organic molecular materials. Our work, in good agreement with recent TR-EPR experimental investigations, showed that optically addressable spin entanglement in radical-bearing molecular materials and architectures is promising for the realization of high-temperature QIP.

Acknowledgements

The authors gratefully acknowledge Prof. Hao Gong (National University of Singapore) and Prof. Jing Liu (Technical Institute of Physics and Chemistry, CAS & Tsinghua University) for helpful discussions. We thank the National Natural Science Foundation of China (Nos. 62164006 and 11564023), Yunnan

Fundamental Research Projects (No. 202101AS070036), Yunnan Local University Joint Special Funds for Basic Research (Nos. 2017FH001-007 and 2018FH001-017), Scientific Research Fund of Yunnan Education Department (Nos. 2020Y0464, 2021Y704, and 2021Y713), and UK Research Councils Basic Technology Program (EP/F041349/1) for funding.

Author details

¹Yunnan Key Laboratory of Metal-Organic Molecular Materials and Devices, Kunming University, Kunming, Yunnan Province, P. R. China. ²Key Laboratory of Yunnan Provincial Higher Education Institutions for Organic Optoelectronic Materials and Devices, Kunming University, Kunming, Yunnan Province, P. R. China. ³School of Physical Science and Technology, Kunming University, Kunming, Yunnan Province, P. R. China. ⁴Yunnan Ocean Organic Optoelectronic Technology Ltd, 650214 Kunming, Yunnan Province, P. R. China. ⁵UCL Institute for Materials Discovery, University College London, Malet Place, London WC1E 7JE, UK

Author contributions

W.W., T.Z., and H.W. contributed to the conception of the paper. L.M., J.C., Q.C., and W.W. performed the theoretical analysis. All authors contributed to the drafting of the paper.

Data availability

All the computer code and data that support the findings of this study are available from the corresponding author upon reasonable request.

Conflict of interest

The authors declare competing interests.

Publisher's note

Springer Nature remains neutral with regard to jurisdictional claims in published maps and institutional affiliations.

Received: 1 September 2021 Revised: 23 February 2022 Accepted: 21 March 2022

Published online: 20 May 2022

References

- Arute, F. et al. Quantum supremacy using a programmable superconducting processor. *Nature* **574**, 505–510 (2019).
- Kjaergaard, M. et al. Superconducting qubits: current state of play. *Annu. Rev. Condens. Matter Phys.* **11**, 369–395 (2020).
- Wu, Y. et al. Strong quantum computational advantage using a superconducting quantum processor. *Phys. Rev. Lett.* **127**, 180501 (2021).
- Raman, K. V. et al. Interface-engineered templates for molecular spin memory devices. *Nature* **493**, 509–513 (2013).
- Filidou, V. et al. Ultrafast entangling gates between nuclear spins using photoexcited triplet states. *Nat. Phys.* **8**, 596–600 (2012).
- Bayliss, S. L., Laorenza, D. W., Mintun, P. J., Diler, B. & Awschalom, D. D. Optically addressable molecular spins for quantum information processing. *Science* **307**, 1309–1312 (2020).
- Wang, Y. X., Liu, Z., Fang, Y. H., Zhou, S. & Gao, S. Coherent manipulation and quantum phase interference in a fullerene-based electron triplet molecular qutrit. *NPJ Quantum Inf.* **7**, 32–40 (2021).
- Stoneham, A. M., Fisher, A. J. & Greenland, P. T. Optically driven silicon-based quantum gates with potential for high-temperature operation. *J. Phys. Condens. Matter* **15**, 447–451 (2003).
- Gaita-Ariño, A., Luis, F., Hill, S. & Coronado, E. Molecular spins for quantum computation. *Nat. Chem.* **11**, 301–309 (2019).
- Warner, M. et al. Potential for spin-based information processing in a thin-film molecular semiconductor. *Nature* **503**, 504–508 (2013).
- Atzori, M. et al. Room-temperature quantum coherence and rabi oscillations in vanadyl phthalocyanine: Toward multifunctional molecular spin qubits. *J. Am. Chem. Soc.* **138**, 2154–2157 (2016).
- Rugg, B. K. et al. Photodrivn quantum teleportation of an electron spin state in a covalent donor–acceptor–radical system. *Nat. Chem.* **11**, 981–986 (2019).

13. Ferrando-Soria, J. et al. A modular design of molecular qubits to implement universal quantum gates. *Nat. Commun.* **7**, 11377 (2016).
14. Gao, Y., Zhang, H., Shuang, S. & Dong, C. Visible-light-excited ultralong-lifetime room temperature phosphorescence based on nitrogen-doped carbon dots for double anticounterfeiting. *Adv. Opt. Mater.* **8**, 1901557 (2020).
15. Teki, Y., Tamekuni, H., Takeuchi, J. & Miura, Y. First evidence for a uniquely spin-polarized quartet photoexcited state of a π -conjugated spin system generated via the ion-pair state. *Angew. Chem. Int. Ed.* **45**, 4666–4670 (2006).
16. Yamauchi, S. Recent developments in studies of electronic excited states by means of electron paramagnetic resonance spectroscopy. *Bull. Chem. Soc. Jpn* **77**, 1255–1268 (2004).
17. Forbes, M. D. E., Jarocha, L. E., Sim, S. & Tarasov, V. F. Time-resolved electron paramagnetic resonance spectroscopy: history, technique, and application to supramolecular and macromolecular chemistry. *Adv. Phys. Org. Chem.* **47**, 1–83 (2013).
18. Rane, V. & Das, R. Distance dependence of electron spin polarization during photophysical quenching of excited naphthalene by TEMPO radical. *J. Phys. Chem. A* **119**, 5515–5523 (2015).
19. Hussain, M. et al. Intersystem crossing in naphthalenediimide-oxoverdazyl dyads: synthesis and study of the photophysical properties. *Chem. Eur. J.* **25**, 15615–15627 (2019).
20. Tripathi, A. K., Rane, V., Kundu, S. & Das, R. A phenomenological scheme for reversed quartet mechanism of electron spin polarization in covalently linked systems of chromophore and free radical: determination of magnitude of polarization and application to pyrene-TEMPO linked molecules. *J. Chem. Phys.* **151**, 154305 (2019).
21. Franco, L. et al. TE-EPR of single and double spin labelled C60 derivatives: observation of quartet and quintet excited states in solution. *Mol. Phys.* **104**, 1543–1550 (2006).
22. Asano-Someda, M. et al. Intramolecular energy transfer in a covalently linked copper(II) porphyrin–free base porphyrin dimer: novel spin polarization in the energy acceptor. *J. Phys. Chem. A* **103**, 6704–6714 (1999).
23. Divincenzo, D. P., Bacon, D., Kempe, J., Burkard, G. & Whaley, K. B. Universal quantum computation with the exchange interaction. *Nature* **408**, 339–342 (2000).
24. Kloeffel, C. & Loss, D. Prospects for spin-based quantum computing in quantum dots. *Annu. Rev. Condens Matter Phys.* **4**, 51–81 (2013).
25. Medford, J. et al. Self-consistent measurement and state tomography of an exchange-only spin qubit. *Nat. Nanotechnol.* **8**, 654–659 (2013).
26. Matsumoto, T. & Teki, Y. Theoretical study of dynamic electron-spin-polarization via the doublet-quartet quantum-mixed state (II). Population transfer and magnetic field dependence of the spin polarization. *Phys. Chem. Chem. Phys.* **14**, 10178–10186 (2012).
27. Takemoto, Y. & Teki, Y. Unique dynamic electron-spin polarization and spin dynamics in the photoexcited quartet high-spin state of an acceptor–donor–radical triad. *ChemPhysChem* **12**, 104–108 (2011).
28. Teki, Y., Matsumoto, T. Theoretical study of dynamic electron-spin-polarization via the doublet-quartet quantum-mixed state and time-resolved ESR spectra of the quartet high-spin state. *Phys. Chem. Chem. Phys.* **13**, 5728 (2011).
29. Kandrashkin, Y. & Van Der Est, A. Electron spin polarization of the excited quartet state of strongly coupled triplet–doublet spin systems. *J. Chem. Phys.* **120**, 4790–4799 (2004).
30. Kandrashkin, Y. & Van Der Est, A. Light-induced electron spin polarization in rigidly linked, strongly coupled triplet–doublet spin pairs. *Chem. Phys. Lett.* **379**, 574–580 (2003).
31. Wu, W. Exchange interaction between the triplet exciton and the localized spin in copper-phthalocyanine. *J. Chem. Phys.* **140**, 224301 (2014).
32. Breuer, H.-P. & Petruccione, F. *The Theory of Open Quantum Systems* (Oxford Univ. Press, 2002).
33. Nolden, O. et al. Excitation energy transfer and exchange-mediated quartet state formation in porphyrin-trityl systems. *Chemistry (Weinheim an der Bergstrasse, Germany)* **27**, 2683 (2021).
34. Scully, M. O. & Zubairy, M. S. *Quantum Optics* (Cambridge Univ. Press, 1997).
35. Sloop, D. J., Yu, H. L., Lin, T. S. & Weissman, S. Electron spin echoes of a photoexcited triplet: pentacene in p-terphenyl crystals. *J. Chem. Phys.* **75**, 3746–3757 (1981).
36. Stoll, S. CW-EPR spectral simulations: Solid state. *Meth. Enzymol.* **563**, 121–142 (2015).
37. Warner, M. et al. Spin-based diagnostic of nanostructure in copper phthalocyanine-C₆₀ solar cell blends. *ACS Nano* **6**, 10808–10815 (2012).
38. Blank, A. & Levanon, H. Triplet line shape simulation in continuous wave electron paramagnetic resonance experiments. *Concepts Magn. Reson. A: Bridg. Educ. Res.* **25**, 18–39 (2005).
39. Misra, S. K. *Multifrequency Electron Paramagnetic Resonance: Theory and Applications* (John Wiley & Sons, 2011).
40. Ishii, K., Hirose, Y. & Kobayashi, N. Selective population from the excited multiplet states to the triplet ground state in a phthalocyanine: a new concept for controlling magnetic properties by photoexcitation. *J. Am. Chem. Soc.* **120**, 10551–10552 (1998).